Measurement of the birefringence variation induced by dihydrogen diffusion into a polarization-maintaining fiber

Mohamed Aazi, Damien Kinet, Claude Renaut, Johan Bertrand, Jean-Louis Auguste, Patrice Mégret, Georges Humbert

Measurement of the birefringence variation induced by dihydrogen diffusion into a polarization maintaining fiber

MOHAMED AAZI[1,2], DAMIEN KINET[2], CLAUDE RENAUT[3], JOHAN BERTRAND[4], JEAN-LOUIS AUGUSTE[1], PATRICE MÉGRET[2,*], AND GEORGES HUMBERT[1,*]

[1] XLIM Research Institute, UMR 7252 CNRS / Limoges University, 123 av. A. Thomas, Limoges, France
[2] Electromagnetism and Telecommunication Department, Faculty of Engineering, University of Mons, Boulevard Dolez 31, 7000 Mons, Belgium
[3] Andra, French National Radioactive Waste Management Agency, Centre de Meuse / Haute-Marne - Route départementale 960 - BP 9 - 55290 Bure, France
[4] Andra, French National Radioactive Waste Management Agency, Parc de la Croix Blanche, 1-7 rue J. Monnet, Chatenay- Malabry, France
[*] Corresponding authors: georges.humbert@xlim.fr, patrice.megret@umons.ac.be

Compiled January 11, 2023

We report continuous measurements of the transmission spectrum of a fiber loop mirror (FLM) interferometer composed of a panda-type polarization maintaining (PM) optical fiber during the diffusion of dihydrogen (H_2) gas into the fiber. Birefringence variation is measured through the wavelength shift of the interferometer spectrum when the PM fiber is inserted into a gas chamber with H_2 concentration from 1.5 % (vol) to 3.5 % (vol) at 75 bar and 70 °C. The measurements correlated with simulation results of H_2 diffusion into the fiber lead to a birefringence variation of -4.25×10^{-8} per mol/m^3 of H_2 concentration in the fiber, with a birefringence variation as low as -9.9×10^{-8} induced by 0.031 µmol/m of H_2 dissolved in the single-mode silica fiber (for 1.5 % (vol)). These results highlight a modification of the strain distribution in the PM fiber, induced by H_2-diffusion, leading to a variation of the birefringence that could deteriorate the performances of fiber devices or improve H_2 gas sensors.

http://dx.doi.org/10.1364/ao.XX.XXXXXX

The diffusion of H_2 gas into optical fibers has been thoroughly studied during the development of the fiber Bragg gratings [1], due to the large improvement of the photosensitivity to UV radiations of standard single-mode telecommunication fibers (SMF) when the fiber was exposed to high-pressure H_2 for several days or even weeks [2]. Knowledge of H_2 concentration in the fiber is important for controlling the photosensitivity, the fiber losses, the modification of photo-elastic properties and the augmentation of the refractive index leading to variations of the properties of fiber Bragg grating based components after manufacturing [3–5]. More recently, Kong *et al.* have developed an UV-post-processing technique based on the diffusion of H_2 into an polarization-maintaining (PM) SMF for locally modifying the acoustic velocity coefficient (by ≈2 %), leading to a Brillouin frequency shift up to −320 MHz, with a Brillouin frequency shift around −2 % per wt% of OH level [6]. They demonstrated the possibility to use this technique to tailor the acoustic velocity along a fiber for improving the suppression of the parasitic stimulated Brillouin scattering in a fiber amplifier. Delepine-Lesoille *at al.* have demonstrated Brillouin optical time-domain analyses of H_2 diffusion into a SMF, in distributed sensing configuration, with a Brillouin frequency shift of about 0.21 MHz/% of H_2 concentration in the fiber [7]. Additional experiments based on simultaneous Brillouin and Rayleigh backscattering measurements during H_2 out-gassing from H_2-loaded SMF (at saturation) have demonstrated a variation of the acoustic velocity of 5.2 m/s per % mol of H_2 dissolved in silica and of the refractive index of silica about 9.7×10^{-4} RIU per % mol of H_2 dissolved in silica [8]. These results allow the development of distributed fiber sensors for remote monitoring of slow variation of H_2 concentration in H_2 rich atmosphere, as for high level and long-lived intermediate level radioactive waste repositories. In contrast to most H_2 fiber sensors that are based on a deposited thin layer of a sensitive material (ex. Palladium (Pd) and tungsten oxide WO_3 [9–13]), raw fiber based distributed sensors offer remote, robust, long-term, and H_2 sensing into long-range structures in harsh and explosive conditions. They do not undergo delamination or the cracking of the sensitive layer that could lead to severe stability problems [14, 15]. However, SMF suffers from a low H_2 sensitivity, as the variation of the Brillouin frequency is about 21 MHz for a hydrogenation saturation at 25 °C and 150 bar. In the prospect to gain in sensitivity while protecting the sensing material to external deteriorations, we have demonstrated that the insertion of Pd particles inside the stress applying parts (SAP) of a Panda-type PM-SMF leads to a variation of the fiber birefringence during H_2 diffusion [16]. This modified fiber improved the wavelength shift of the transmission spectrum of a Fiber Loop Mirror (FLM) interferometer by 32 % and reduced the response time by 50 %, in comparison to the same PM-SMF without Pd particles. Both PM fibers were inserted within a FLM interferometer and put in a gas chamber fully filled (100 %) of H_2 gas. Besides, in comparison with a FBG written in a SMF (also inserted in the gas chamber), we observed that both PM fibers

exhibit a faster response time and a larger wavelength shift. These results associated with the large Brillouin frequency shift (−320 MHz) reported by Kong *at al.* [6] in a PM-SMF (against 21 MHz in a SMF [7]) highlight a modification of the strain distribution in the PM-SMF, induced by H_2-diffusion, leading to significant variation of the fiber birefringence that could deteriorate the performances of devices or improve H_2 gas sensors.

In this paper, we explore this birefringence variation in a simple commercial PM-SMF (Thorlabs XP-1550, composed of boron doped SAP). We have designed an experimental setup to continuously measure the birefringence variation of PM fibers during diffusion of H_2 under controlled pressure and temperature. Different H_2 concentrations from 0.5 to 3.5 % (vol) at 75 bar have been applied showing a birefringence variation of about -4.2×10^{-8} per mol/m^3 of H_2 dissolved in silica.

The experimental setup used for continuously measuring the diffusion of H_2 into an PM-SMF, shown in Figure 1(a), is composed of a hermetic gas chamber (of 2.5 L volume) with two channels for hydrogen (H_2) gas and nitrogen (N_2) gas flowing with controlled pressure and temperature.

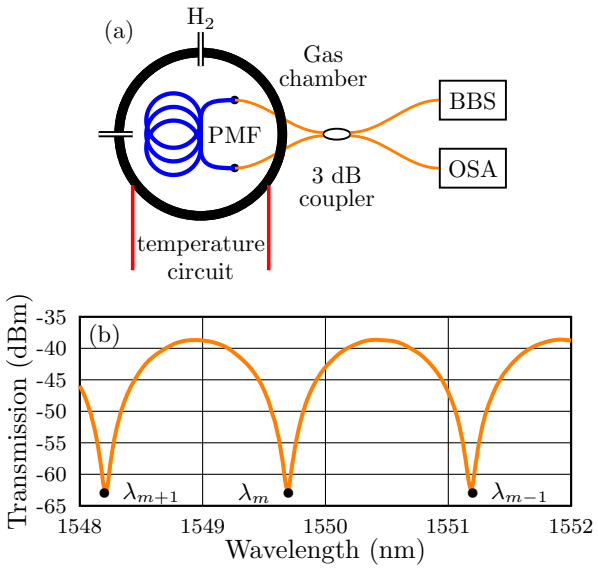

Fig. 1. (a) Experimental setup of the FLM interferometer hydrogen monitoring system based on commercial PM Panda fiber, BBS = broadband source, OSA = optical spectrum analyzer, (b) Transmission spectrum of the interferometer with a fiber length of 4 m.

The PM-SMF, spliced between two pigtails of SMF, is inserted into the chamber and connectorized through hermitic optical connectors, to the arms of a single-mode fiber based 3 dB-coupler to form a FLM interferometer. A broadband light source (BBS) with a central wavelength around 1550 nm and a spectral bandwidth of 100 nm is used with an optical spectrum analyzer (OSA, wavelength resolution of 0.05 nm) for measuring the transmission spectrum of the FLM. The PM fiber is a Panda-type fiber (Thorlabs XP-1550) with an inner cladding diameter of 125 µm and a core diameter of 8 µm. The stress-applying parts (SAP) are composed of boron-doped silica with a diameter of 36.5 µm distanced by 4.5 µm from the germanium-doped core center. The fiber has a core/cladding index difference of 5.5×10^{-3} and a SAP/cladding index difference value of -12×10^{-3}. A FLM interferometer is a sensitive configuration to many physical parameters, and in particlular to the birefringence of a PM-fiber [17, 18]. The transmission spectrum $T(\lambda)$ of the FLM (Fig. 1(b)) depends on the length L and on the group birefringence B of the PM fiber, as the incident light from the BBS is split into two beams of clockwise and anticlockwise propagations. Each of the resultant beam is decomposed into two polarization components after it travels through the high birefringence fiber. The counter-propagating beams recombine at the output of the coupler and exhibits interference according the phase difference induced by the birefringence. The output spectrum can be expressed, as a sine-square function relative to the incident light wavelength by [17]:

$$T(\lambda) = \sin^2 \frac{\pi B L}{\lambda} \quad \textbf{(1)}$$

where λ is the center wavelength of the light source. The dip wavelength λ_m in the interferometer spectra (Fig. 1(b)) corresponds to a phase shift of $2m\pi$ (m is an integer) and is described as:

$$\lambda_m = \frac{L}{2m} B \quad \textbf{(2)}$$

The measurement of the shift of the transmission spectrum (i.e., dip wavelengths λ_m) enables to sense tiny variations of the birefringence (B). The sensitivity is limited by the limit of detection of the wavelength shift that depends on the period of the interferences, and the resolution of the OSA. To find the best configuration, we have evaluated the sensitivity of the system at ambient temperature with several lengths of PM fiber (0.6 m, 4 m and 10 m) and with different measurement resolutions (0.2 nm, 0.1 nm and 0.05 nm). The FLM spectra with a PM fiber length of 0.6 m, 4 m and 10 m are composed of 7, 40, and 100 dips, respectively, in a wavelength range of 70 nm. A resolution of 0.05 nm and a fiber length of 4 m (FWHM of 1.32 nm, Figure 1(b)) were selected for ensuring an efficient tracking of the wavelength dips, with measurements each minute. By Eq. (2), the measured birefringence of the PM fiber is estimated to be 4.33×10^{-4} around 1550 nm at ambient temperature and pressure. The diffusion of H_2 inside the optical fiber is monitored by measuring each minute the transmission spectrum of the FLM and more precisely by tracking the shift of the dips. Even if the wavelength shift is not a direct measurement of the birefringence variation, it is an indirect and accurate means to sense H_2 diffusion into the fiber. The temporal evolution of the H_2 diffusion through the cross-section of an optical fiber (from the external boundary to the center) is expressed by the Fick's law, leading to Eq. (3) for the H_2 concentration $[H_2]$ [19]:

$$\frac{\partial [H_2]}{\partial t} = D \left(\frac{\partial^2 [H_2]}{\partial r^2} + \frac{1}{r} \frac{\partial [H_2]}{\partial r} \right) \quad \textbf{(3)}$$

where D is the diffusion coefficient of H_2 into SiO_2, expressed as [20] for silica:

$$D = 2.83 \times 10^8 \exp\left(-\frac{40\,190}{RT} \right) \quad \textbf{(4)}$$

where R is the universal gas constant and T the absolute temperature. It is worth to note that H_2 diffusion does not depend on the gas pressure, but on the temperature. Higher temperatures and smaller fiber diameters lead to faster H_2 diffusion in silica. The concentration of H_2 in silica at saturation ($[H_2]_{sat}$) is obtained from the solubility S of H_2 into SiO_2 by the relation [20]:

$$[H_2]_{sat} = \frac{p_{H_2} S}{N_A} = \frac{p_{H_2}}{N_A} 71 \times 10^{21} \exp\left(\frac{8900}{RT} \right) \quad \textbf{(5)}$$

with N_A the Avogadro constant, and p_{H_2} the partial pressure of H_2. It is clear that the concentration of H_2 at saturation is larger with lower temperature and/or higher pressure. Therefore, the temperature and the pressure of H_2 in the gas chamber were set at 70 °C and 75 bar, respectively. This enables a rather fast H_2 diffusion in the fiber samples until saturation with measurable H_2 concentration, that leads to the following experimental protocol. Measurement with nitrogen (N_2) gas was realized to calibrate the system. As shown in Figure 2(a), the chamber was initially filled with ambient air at room temperature (17.5 °C), then N_2 was inserted at 60 bar (during 7 hours, for checking the hermiticity of the chamber), and finally, the temperature and N_2 pressure were increased up to 70 °C and 75 bar, respectively. These conditions were maintained during 67 h to enable slow dynamic measurements. Then the gas was released and the temperature was dropped down to room temperature. Continuous measurements of the transmission spectrum of the FLM allow us to quantify a linear shift of the wavelength dips of 0.01 nm/h (Figure 2(b)) corresponding to the drift of the measurement system.

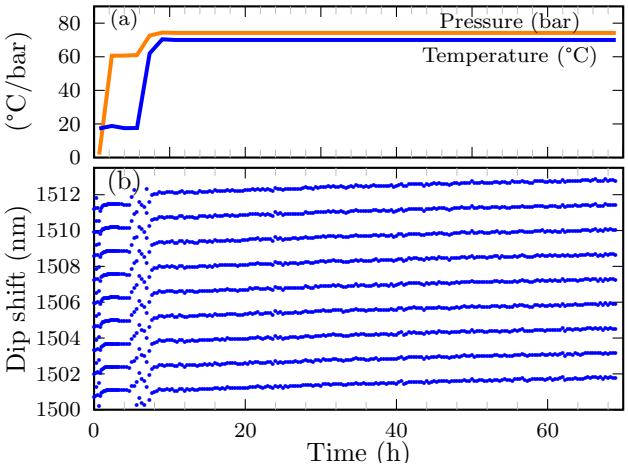

Fig. 2. (a) Pressure and temperature variations, and (b) wavelength of spectrum dips during the calibration measurements with N_2-gas.

To monitor the diffusion of H_2 into the PM fiber, at different concentrations, the chamber was initially filled with N_2 gas ($p = 60$ bar at room temperature, 18.5 °C) during few hours to check again the hermiticity. Then, H_2 was injected in the gas chamber at different concentrations, next, the temperature and the pressure of N_2 were increased to 70 °C and 75 bar, respectively. Finally, after 67 h in these conditions, the chamber was purged, opened and the PM fiber was removed and replaced by a virgin one. This protocol was used for measuring the diffusion of H_2 at a concentration of 0.5 %, 1.5 %, 2.5 % and 3.5 % (vol %). Figure 3 shows the evolution of the dips wavelength of the FLM measured on-line each minute during this hydrogenation protocol for a gas chamber filled with N_2 gas mixed with 1.5 % (vol) of H_2 gas. The normalized wavelength shift $(\lambda - \lambda_0)/\lambda_0$, with λ_0 the wavelength at the beginning of the hydrogenation stage, is calculated for each interference dips of the FLM transmission spectra leading to a mean curve (see Supplement 1, Fig. S2(b)). The mean normalized wavelength shift of the interference dips is also calculated for the calibration measurement with N_2 (see Supplement 1, Fig. S2(a)). The experiment and these calculations are repeated for other H_2 concentrations (see Supplement 1, Fig. S1) leading to the mean normalized wavelength shift for the three concentrations (see Supplement 1, Fig. S2).

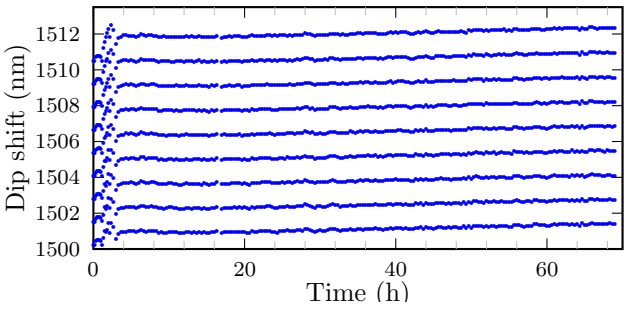

Fig. 3. Wavelength of spectrum dips during the hydrogenation protocol with 1.5 % (vol) of H_2-gas.

The normalized wavelength shift of the average interference dips versus the hydrogenation time is plotted in Figure 4, for different H_2 concentrations. The curves include the correction from the system calibration. They exhibit a continuous shift of the interference dip to shorter wavelengths following an exponential decay until a plateau corresponding to the saturation regime. As the kinetic of H_2 diffusion in this transient regime only depends on the temperature, we have simulated (from Eq. (3)) the normalized diffusion of 100 % of H_2 (at 70 °C) into the center of a silica cylinder 125 µm diameter, and then, fitted the normalized wavelength shift of the average interference dips with this simulation curve by applying, for each concentration, a multiplication factor that corresponds to the mean normalized wavelength shift at saturation (Column 5 in Table 1). Indeed, after 67 h of hydrogenation at 70 °C the normalized concentration of H_2 is about 91.96 % of the saturation stage. As shown in Figure 4, these curves match the measured data emphasizing that the kinetic of H_2 diffusion into the fiber was correctly measured with this apparatus based on a Panda PM-fiber. After 67 h of hydrogenation in these conditions (75 bar and 70 °C), the mean normalized wavelength shift obtained from these curves is summarized in table 1. The mean normalized wavelength shift at saturation (Column 5 in Table 1) is also equal to the measured value (Column 3 in Table 1) divided by 91.96 %.

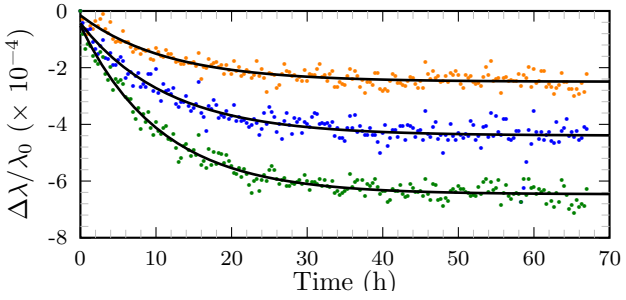

Fig. 4. Normalized wavelength shift of the average interference dips during the hydrogenation protocol with different hydrogen concentrations (orange is 1.5 %, blue is 2.5 %, and green is 3.5 % (vol. %).

The concentration of H_2 in the fiber can be calculated at saturation (Column 4 in Table 1) from Eq. (5) knowing the partial pressures for the different concentrations of H_2, following the hydrogenation protocol. This factor of 91.96 % is also applied to

Table 1. Summary of the results after hydrogenation and computed values.

$[H_2]$	$p(H_2)$	$\frac{\Delta\lambda}{\lambda_0}$ (67 h)	c (sat)	$\frac{\Delta\lambda}{\lambda_0}$ (sat)	c (67 h)	ΔB (67 h)
%	bar	10^{-4}	mol/m^3	10^{-4}	mol/m^3	10^{-7}
1.5	1.06	−2.39	2.76	−2.60	2.54	−0.99
2.5	1.77	−4.23	4.60	−4.60	4.23	−1.70
3.5	2.48	−6.25	6.45	−6.80	5.93	−2.52

c(sat) for obtaining the concentration of H_2 in the fiber at the end of the hydrogenation process (Column 6 in Table 1). It is worth to note that these concentrations correspond to 0.12, 0.21 and 0.29 µmol of H_2 in the 4-meter long Panda fiber, for the different hydrogenation concentrations of 1.5, 2.5 and 3.5 % (vol) of H_2, respectively. Furthermore, these also correspond to a ratio of H_2 in silica of about 0.6×10^{-4}, 1.1×10^{-4}, and 1.5×10^{-4}, respectively. These calculations lead to plotting the mean normalized wavelength shift (at $t_{H_2} = 67$ h) versus the H_2 concentration at the same time (Fig. 5(a)) that is linearly fitted with a slope of -1.05×10^{-4} per mol/m^3 and a standard error of 4.2×10^{-6}. Furthermore, Eq. (2) is linear in B, so that the normalized wavelength shift $\Delta\lambda/\lambda_0$ induced by a birefringence variation ΔB is simply expressed as:

$$\frac{\Delta\lambda(t)}{\lambda_0} = \frac{\lambda(t) - \lambda_0}{\lambda_0} = \frac{\Delta B(t)}{B_0} \tag{6}$$

with B_0 the birefringence at the beginning of the hydrogenation stage, easily computed from the positions of λ_m at the initial time (see Fig. 1(b)). The calculation of B_0 from the measured transmission spectrum of each experiment (at $t_{H_2} = 0$ h) leads to a birefringence variation at $t_{H_2} = 67$ h of about -9.9×10^{-8}, -1.7×10^{-7} and -2.52×10^{-7} respectively. These variations are linearly fitted versus the H_2 concentration in silica (Fig. 5(b)) with a slope of -4.25×10^{-8} per mol/m^3 (with a standard error of 1.16×10^{-9}), which is equivalent to a birefringence variation of -7.43×10^{-8} per % (vol) of H_2 in the chamber (with a standard error of 2.66×10^{-9}).

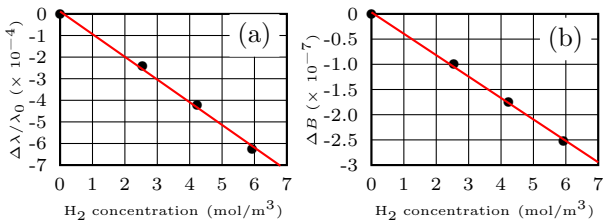

Fig. 5. (a) Normalized wavelength shift of interference dips, and (b) Birefringence variation, versus the concentration of H_2 dissolved in silica.

In conclusion, we have demonstrated continuous monitoring of H_2 diffusion into a commercially available Panda-PM fiber within a FLM interferometer inserted in a gas chamber, with H_2 concentration from 1.5 % (vol) to 3.5 % (vol) at 75 bar and 70 °C. The evolution of the H_2 concentration in the fiber was obtained by correlating the simulation of the normalized diffusion of H_2 in fiber core, with the measurements of the wavelength shift of the FLM transmission spectrum. From these results we have demonstrated a birefringence variation of -4.25×10^{-8} per mol/m^3 of H_2 concentration, with a birefringence variation as low as -9.9×10^{-8} induced by 2.54 mol/m^3 of H_2 dissolved in silica (for 1.5 % (vol)). As this result has been obtained at almost saturation ($t_{H_2} = 67$ h), smaller birefringence variation could be measured during the diffusion of H_2 into the fibre, which is emphasising the sensitivity of this configuration. Furthermore, this configuration does not require any fiber post-processing, fiber functionalization with a sensitive material to H_2, and neither a specific component. It is robust, low-cost, compact, easy to realize and highly compatible with remote monitoring slow leakage of H_2 in harsh environments such as nuclear waste disposals. In addition, this experimental demonstrations offer new insights for developing novel PM fibers with improved H_2 sensitivity.

Funding. Project Modern2020, Euratom research and training program 2014-2018, grant agreement No 662177; French National Radioactive Waste Management Agency (ANDRA).

Disclosures. The authors declare no conflicts of interests.

Data availability. Data underlying the results are not publicly available but may be obtained from the authors upon reasonable request.

Supplemental document. See Supplement 1 for supporting content.

REFERENCES

1. K. O. Hill, Y. Fujii, D. C. Johnson, and B. S. Kawasaki, Appl. Phys. Lett. **32**, 647 (1978).
2. P. J. Lemaire, R. M. Atkins, V. Mizrahi, and W. A. Reed, Electron. Lett. **29**, 1191 (1993).
3. P. L. Swart and A. A. Chtcherbakov, J. Light. Technol. **20**, 1933 (2002).
4. B. Malo, D. C. Johnson, F. Bilodeau, J. Albert, and K. O. Hill, Electron. Lett. **30**, 442 (1994).
5. S. R. Baker, H. N. Rourke, V. Baker, and D. Goodchild, J. Light. Technol. **15**, 1470 (1997).
6. F. Kong and L. Dong, Opt. Express **20**, 27810 (2012).
7. S. Delepine-Lesoille, J. Bertrand, L. Lablonde, and X. Pheron, IEEE Photonics Technol. Lett. **24**, 1475 (2012).
8. S. Leparmentier, J. L. Auguste, G. Humbert, G. Pilorget, L. Lablonde, and S. Delepine-Lesoille, "Study of the hydrogen influence on the acoustic velocity of single-mode fibers by rayleigh and brillouin backscattering measurements," in *SPIE Proceedings*, H. J. Kalinowski, J. L. Fabris, and W. J. Bock, eds. (SPIE, 2015).
9. M. Tabib-Azar, B. Sutapun, R. Petrick, and A. Kazemi, Sensors Actuators B: Chem. **56**, 158 (1999).
10. B. Xu, C. L. Zhao, F. Yang, H. Gong, D. N. Wang, J. Dai, and M. Yang, Opt. Lett. **41**, 1594 (2016).
11. M. Yang, Z. Yang, J. Dai, and D. Zhang, Sensors Actuators B: Chem. **166-167**, 632 (2012).
12. C. Caucheteur, M. Debliquy, D. Lahem, and P. Mégret, IEEE Photonics Technol. Lett. **20**, 96 (2008).
13. Y. Wang, M. Yang, G. Zhang, J. Dai, Y. Zhang, Z. Zhuang, and W. Hu, J. Light. Technol. **33**, 2530 (2015).
14. E. Lee, J. M. Lee, J. H. Koo, W. Lee, and T. Lee, Int. J. Hydrog. Energy **35**, 6984 (2010).
15. F. Greco, L. Ventrelli, P. Dario, B. Mazzolai, and V. Mattoli, Int. J. Hydrog. Energy **37**, 17529 (2012).
16. M. Aazi, M. Kudinova, D. Kinet, J.-L. Auguste, S. Delépine-Lesoille, P. Mégret, and G. Humbert, J. Physics: Photonics **2**, 014005 (2019).
17. Y. Liu, B. Liu, X. Feng, W. Zhang, G. Zhou, S. Yuan, G. Kai, and X. Dong, Appl. Opt. **44**, 2382 (2005).
18. A. N. Starodumov, L. A. Zenteno, D. Monzon, and E. D. L. Rosa, Appl. Phys. Lett. **70**, 19 (1997).
19. P. J. Lemaire, Opt. Eng. **30**, 780 (1991).
20. J. F. Shackelford, P. L. Studt, and R. M. Fulrath, J. Appl. Phys. **43**, 1619 (1972).

FULL REFERENCES

1. K. O. Hill, Y. Fujii, D. C. Johnson, and B. S. Kawasaki, "Photosensitivity in optical fiber waveguides: Application to reflection filter fabrication," Appl. Phys. Lett. **32**, 647–649 (1978).
2. P. J. Lemaire, R. M. Atkins, V. Mizrahi, and W. A. Reed, "High pressure H_2 loading as a technique for achieving ultrahigh UV photosensitivity and thermal sensitivity in GeO2 doped optical fibres," Electron. Lett. **29**, 1191 (1993).
3. P. L. Swart and A. A. Chtcherbakov, "Study of hydrogen diffusion in boron/germanium codoped optical fiber," J. Light. Technol. **20**, 1933–1941 (2002).
4. B. Malo, D. C. Johnson, F. Bilodeau, J. Albert, and K. O. Hill, "Effective index drift from molecular hydrogen diffusion in hydrogen-loaded optical fibres and its effect on bragg grating fabrication," Electron. Lett. **30**, 442–444 (1994).
5. S. R. Baker, H. N. Rourke, V. Baker, and D. Goodchild, "Thermal decay of fiber bragg gratings written in boron and germanium codoped silica fiber," J. Light. Technol. **15**, 1470–1477 (1997).
6. F. Kong and L. Dong, "Precise tailoring of acoustic velocity in optical fibers by hydrogenation and UV exposure," Opt. Express **20**, 27810 (2012).
7. S. Delepine-Lesoille, J. Bertrand, L. Lablonde, and X. Pheron, "Distributed hydrogen sensing with brillouin scattering in optical fibers," IEEE Photonics Technol. Lett. **24**, 1475–1477 (2012).
8. S. Leparmentier, J. L. Auguste, G. Humbert, G. Pilorget, L. Lablonde, and S. Delepine-Lesoille, "Study of the hydrogen influence on the acoustic velocity of single-mode fibers by rayleigh and brillouin backscattering measurements," in *SPIE Proceedings,* H. J. Kalinowski, J. L. Fabris, and W. J. Bock, eds. (SPIE, 2015).
9. M. Tabib-Azar, B. Sutapun, R. Petrick, and A. Kazemi, "Highly sensitive hydrogen sensors using palladium coated fiber optics with exposed cores and evanescent field interactions," Sensors Actuators B: Chem. **56**, 158–163 (1999).
10. B. Xu, C. L. Zhao, F. Yang, H. Gong, D. N. Wang, J. Dai, and M. Yang, "Sagnac interferometer hydrogen sensor based on panda fiber with Pt-loaded WO_3/SiO_2 coating," Opt. Lett. **41**, 1594 (2016).
11. M. Yang, Z. Yang, J. Dai, and D. Zhang, "Fiber optic hydrogen sensors with sol–gel WO_3 coatings," Sensors Actuators B: Chem. **166-167**, 632–636 (2012).
12. C. Caucheteur, M. Debliquy, D. Lahem, and P. Mégret, "Catalytic fiber bragg grating sensor for hydrogen leak detection in air," IEEE Photonics Technol. Lett. **20**, 96–98 (2008).
13. Y. Wang, M. Yang, G. Zhang, J. Dai, Y. Zhang, Z. Zhuang, and W. Hu, "Fiber optic hydrogen sensor based on Fabry–Perot interferometer coated with sol-gel Pt/WO_3 coating," J. Light. Technol. **33**, 2530–2534 (2015).
14. E. Lee, J. M. Lee, J. H. Koo, W. Lee, and T. Lee, "Hysteresis behavior of electrical resistance in Pd thin films during the process of absorption and desorption of hydrogen gas," Int. J. Hydrog. Energy **35**, 6984–6991 (2010).
15. F. Greco, L. Ventrelli, P. Dario, B. Mazzolai, and V. Mattoli, "Micro-wrinkled palladium surface for hydrogen sensing and switched detection of lower flammability limit," Int. J. Hydrog. Energy **37**, 17529–17539 (2012).
16. M. Aazi, M. Kudinova, D. Kinet, J.-L. Auguste, S. Delépine-Lesoille, P. Mégret, and G. Humbert, "Impact of H_2 gas on disruptive birefringence optical fibers with embedded palladium particles for developing robust sensors," J. Physics: Photonics **2**, 014005 (2019).
17. Y. Liu, B. Liu, X. Feng, W. Zhang, G. Zhou, S. Yuan, G. Kai, and X. Dong, "High-birefringence fiber loop mirrors and their applications as sensors," Appl. Opt. **44**, 2382–2390 (2005).
18. A. N. Starodumov, L. A. Zenteno, D. Monzon, and E. D. L. Rosa, "Fiber sagnac interferometer temperature sensor," Appl. Phys. Lett. **70**, 19–21 (1997).
19. P. J. Lemaire, "Reliability of optical fibers exposed to hydrogen: prediction of long-term loss increases," Opt. Eng. **30**, 780 (1991).
20. J. F. Shackelford, P. L. Studt, and R. M. Fulrath, "Solubility of gases in glass. II. He, Ne, and H2 in fused silica," J. Appl. Phys. **43**, 1619–1626 (1972).